Chemical Engineering Science 77 (2012) 150–156

Contents lists available at SciVerse ScienceDirect

Chemical Engineering Science

journal homepage: www.elsevier.com/locate/ces

Characterization of intermediate stages in the precipitation of hydroxyapatite at 37 °C

Filipa Castro [a,*], António Ferreira [a], Fernando Rocha [b], António Vicente [a], José António Teixeira [a]

[a] IBB—Institute for Biotechnology and Bioengineering, Centre for Biological Engineering, University of Minho, Campus de Gualtar, 4710-057 Braga, Portugal
[b] LEPAE—Laboratory for Process, Environmental and Energy Engineering, Faculty of Engineering of the University of Porto, Rua Roberto Frias, s/n, 4200-465 Porto, Portugal

ARTICLE INFO

Article history:
Received 9 September 2011
Received in revised form
12 January 2012
Accepted 24 January 2012
Available online 6 February 2012

Keywords:
Precipitation
Batch
Calcium phosphate
Supersaturation
Morphology
Aggregation

ABSTRACT

Precipitation of hydroxyapatite $Ca_5(PO_4)_3OH$ (HAp) was carried out by mixing a saturated calcium hydroxide aqueous solution with an orthophosphoric acid aqueous solution at 37 °C. In order to promote optimal conditions for the production of HAp with high yields, mixing of the reaction medium was assured by a novel metal stirrer. Different experimental conditions were studied varying the mixing Ca/P molar ratio from 1 to 1.67. After process optimization, a suspension of HAp particles with pH close to 7 was obtained for a mixing molar ratio Ca/P=1.33. The precipitation process was then characterized as a function of pH and calcium concentration, revealing the existence of three different stages. The precipitate formed in each stage was characterized by scanning electron microscopy and X-ray diffraction.

1. Introduction

Calcium phosphates are widely used in biomedical applications, since their chemical composition is roughly equivalent to that of the inorganic matrix of human bone. Among them, special attention has been paid to hydroxyapatite $Ca_5(PO_4)_3OH$ (HAp), due to its exceptional biocompatibility, bioactivity and osteoconductivity (He and Huang, 2007).

HAp is usually produced from wet chemical synthesis, due to its simplicity, low cost, and easy application in industrial production (Liu et al., 2001). Depending on the precipitation conditions, like stirring speed, reactants addition rate, Ca/P molar ratio, reaction temperature and pH, one can obtain HAp particles with different morphology, size and purity (Elliot, 1994; Ferraz et al., 2004).

Several methods have been used, namely using nitrate, ammonium and phosphate ions that in addition to be polluting agents also require additional experimental steps to eliminate by-products resulting from the reaction. This paper refers to a simple and non-polluting method. It consists in preparing HAp from neutralization between calcium hydroxide with orthophosphoric acid:

$$5Ca(OH)_2+3H_3PO_4\rightarrow Ca_5(PO_4)_3OH\downarrow+9H_2O \quad (1)$$

However, it is difficult to control the reaction conditions for the powder desired characteristics, since calcium hydroxide is slightly soluble in water and the state of the orthophosphate ions depends on pH. To overcome this limitation, most of the works have focused on the control of pH to favor the presence of the PO_4^{3-} ions and thus avoid the formation of other calcium phosphates. In Osaka et al. (1991) and Bernard et al. (2000) works, the authors studied the influence of the acid addition rate on the HAp powder properties and on the calcium hydroxide dissolution rate, respectively, demonstrating that maintenance of an alkaline reaction medium is fundamental to favor the formation of stoichiometric HAp. Nevertheless, for the synthesis of HAp for medical purposes, there is a concern in preparing HAp under conditions that are more conductive to the survival of cells. The preparation has to follow specific criteria, namely about pH and temperature conditions (Kumta et al., 2005).

In this work we report a simple methodology for the synthesis of HAp from diluted solutions at 37 °C. For that, a saturated calcium hydroxide aqueous solution was mixed with an orthophosphoric acid aqueous solution, without maintaining a fixed pH. By this way, a homogeneous solution of hydroxide and calcium ions shall be obtained, avoiding the formation of local concentration gradients, while maximizing HAp precipitation process. Further, reagents were mixed by a novel metal stirrer, designed in order to obtain an efficient and intense mixing of the reaction medium. The influence of the mixing Ca/P molar ratio on the powder properties and on the final pH value was studied, the optimum conditions being derived for obtaining stable HAp

* Corresponding author. Tel.: +351 253 604400; fax: +351 253 678986.
E-mail address: fcastro@deb.uminho.pt (F. Castro).

0009-2509/$ - see front matter © 2012 Elsevier Ltd. All rights reserved.
doi:10.1016/j.ces.2012.01.058

nanoparticles under near-physiological conditions of temperature and pH, i.e., HAp particles suitable for bone substitution application. Finally, the intermediate stages for the optimized HAp precipitation process were described.

2. Experimental procedure

2.1. HAp precipitation

Precipitation was carried out in a cylindrical batch reactor (Fig. 1) made of glass, with 100 mm in diameter and 250 mm in height, where temperature was regulated by a water jacket and a thermostatic bath maintained at 37 °C. The agitation was assured by a novel metal stirrer (Fig. 1) and kept at 270 rpm.

HAp was synthesized by the mixing of equal volumes (0.5 dm^3) of a saturated calcium hydroxide (Riedel-de Haën, 96%) aqueous solution and an orthophosphoric acid (Pronalab, 85%) aqueous solution, with different mixing Ca/P molar ratios (1, 1.33 and 1.67).

A 19.3 mmol/dm^3 calcium hydroxide aqueous solution, that is, a saturated calcium hydroxide aqueous solution at $T=37$ °C (Perry and Green, 1997) was prepared. To facilitate the dissolution of calcium hydroxide, the solution was agitated in a closed vessel for 24 hours at 500 rpm, and at 25 °C, as its solubility decreases with the increase of temperature (Johannsen and Rademacher, 1999). Calcium concentration was then confirmed by EDTA (Riedel-de Haën, 99%) titration. Both saturated calcium hydroxide aqueous solution and orthophosphoric acid aqueous solution were prepared with ultra pure water, and ionic force was adjusted by the addition of 6 ml of KCl (Panreac, 99.5%) 4M solution.

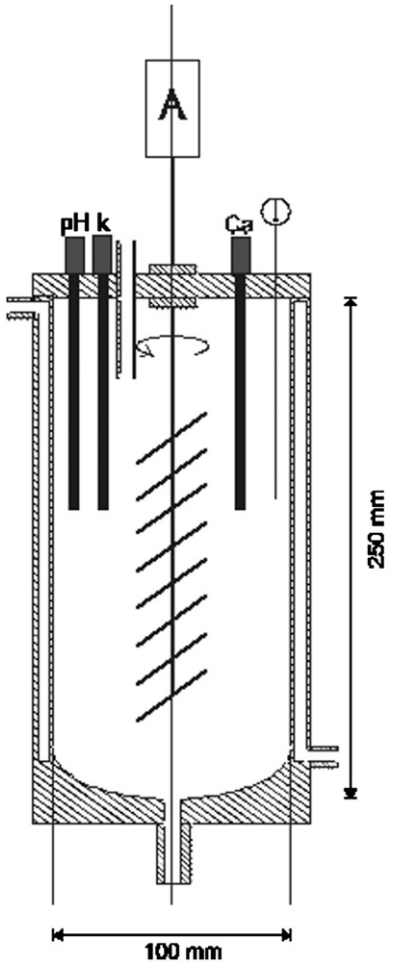

Fig. 1. Experimental precipitation apparatus.

Precipitation started by the quick addition ($\approx$26 ml/s) of the orthophosphoric acid aqueous solution to the saturated calcium hydroxide aqueous solution. The concentration of the orthophosphoric acid aqueous solution varied from 11.5 mmol/dm^3 to 19.3 mmol/dm^3, so as to obtain different mixing Ca/P molar ratios.

Calcium concentration, pH, temperature and conductivity were continuously measured (inolab pH/cond level 3, WTW) and recorded for about 6 hours. The different electrodes were calibrated with buffer solutions. pH calibration was made with two buffer solutions (Hanna Instruments) with pH=7.01 and pH=10.01 at 25 °C. Regarding calcium electrode (inolab Ca 800, WTW), its calibration was done using standard solutions of 5 and 50 ppm of calcium. Those were prepared from $CaCl_2$ (Merck proanalysis, 98%) and ionic force was adjusted by the addition of 6 ml of KCl (Panreac, 99.5%) 4 M solution per 500 ml of standard solution.

2.2. HAp characterization

Samples were withdrawn at different time intervals, filtered (membrane of 0.2 μm pore size, Gelman Sciences, USA) and dried at $T=60$ °C during 24 h. The particles obtained were then characterized by XRD (PanAlytical X'Pert PRO Alfa-1 diffractometer with $\lambda_{CuK\alpha}=1.54056$ Å), FTIR (Bomem MB-154S) and SEM (FEI Quanta 400FEG ESEM/EDAX Genesis X4M with an accelerating voltage of 15 kV and 20 kV), where samples were covered by a 10 nm layer of gold. For particle size distribution (LS 230, Beckman Colter), cryo-SEM (JEOL JSM 6301 F/Oxford INCA Energy 350/Gatan Alto 2500 with an accelerating voltage of 15 kV) and zeta potential measurements (Malvern Nano ZetaSizer), suspensions were collected at the end of each experiment and directly analyzed. As to the Ca/P molar ratio of the final product, total phosphorus was quantified by the ascorbic acid method (spectrophotometer PG Instruments Ltd. T60 UV/VIS) and calcium was measured by atomic absorption spectroscopy (spectrometer GBC 932Plus).

3. Experimental results and discussion

3.1. HAp precipitation process

From a thermodynamic point of view, the existing conditions favor the spontaneous precipitation of HAp, since it is the most stable calcium phosphate for pH between 4 and 12 at body temperature (Elliot, 1994). But considering the kinetics it does not mean that HAp is the only calcium phosphate to precipitate (Koutsopoulos, 2002). Thus, to reduce the influence of the kinetic factors, precipitation of HAp was performed from diluted solutions so as to obtain low supersaturations. Indeed, at low supersaturations homogeneous formation of the most stable phase is to be expected as the solution would be saturated or even undersaturated with respect to the other phases (van Kemenade and de Bruyn, 1987). As it was referred above, calcium hydroxide is slightly soluble in water and generally a suspension with aggregates of undissolved calcium hydroxide is obtained. Therefore, through the use of diluted solutions it is intended to get a homogeneous solution of hydroxide and calcium ions in order to avoid the formation of local concentration gradients, so allowing a better control of the reaction conditions.

3.2. HAp precipitation process for mixing molar ratios Ca/P=1, 1.33 and 1.67

pH of the reaction medium was continuously measured during the precipitation process for all the operating conditions (Fig. 2).

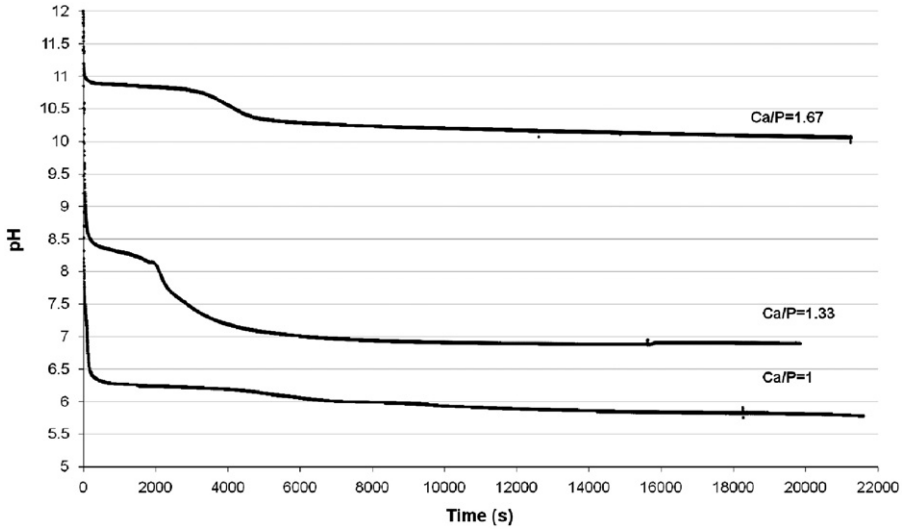

Fig. 2. Variation of pH with time during HAp precipitation at $T=37$ °C for different mixing Ca/P molar ratios.

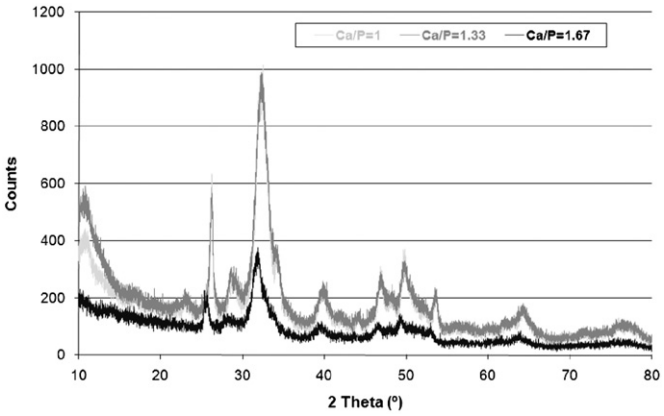

Fig. 3. XRD patterns of the products formed during HAp precipitation at $T=37$ °C for different mixing Ca/P molar ratios.

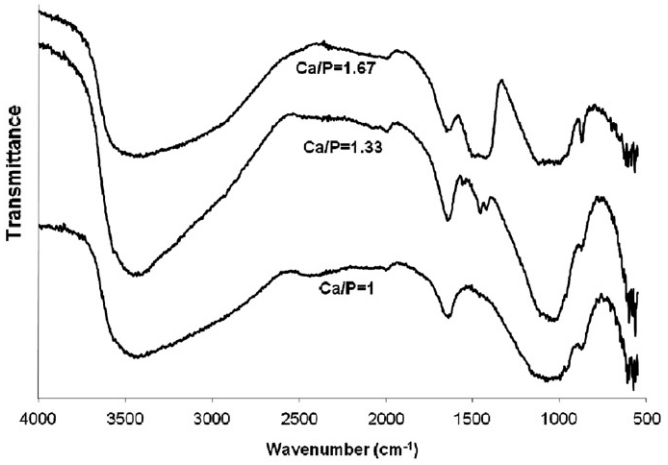

Fig. 4. FTIR spectra of the products formed during HAp precipitation at $T=37$ °C for different mixing Ca/P molar ratios.

Initial pH, corresponding to the pH of the saturated aqueous solution of calcium hydroxide, was high (>12) and similar to the expected value (Safavi and Nakayama, 2000). After the addition of the orthophosphoric acid aqueous solution, pH decreased and reached a plateau at approximately 10.8, 8.2 and 6.2 for Ca/P=1.67, 1.33 and 1, respectively. Then, pH decreased slowly and stabilized, showing that the majority of the reaction is completed after, approximately, 10000 s. Further, for Ca/P=1.33, pH stabilized near 7, as intended.

XRD patterns of the final products are shown in Fig. 3. Formation of single-phased HAp was verified, more specifically nanocrystalline HAp due to the presence of broad diffraction peaks, namely at 26° 2θ and 30 to 34° 2θ (Tadic et al., 2002; Venkateswarlu et al., 2010). Besides, XRD patterns obtained are similar to XRD patterns of biological apatites, which also present broad diffraction peaks, characteristic of small crystallites (Marković et al., 2011).

Functional groups of HAp were confirmed by FTIR analysis (Fig. 4). Bands for the hydroxyl group, OH^-, and for the phosphate group, $PO4^{3-}$, although not well resolved, were exhibited. Moreover, spectra exhibit a broad band from approximately 3700 to 3000 cm^1 and a peak at 1643 cm^{-1}, revealing the existence of adsorbed water on the HAp particles, which can be justified by the low drying temperature (60 °C) and the absence of a ripening (ageing) treatment (Koutsopoulos, 2002; Osaka et al., 1991; Zhou et al., 2008). The peak assigned to stretching mode of OH^- is weak in the spectrum of the product obtained with a mixing molar ratio Ca/P=1.33 (around 3571 cm^{-1}) and is not visible in the other spectra. This can be due to the overlap with the broad peak of the adsorbed water on HAp particles (Ma and Zhu, 2009). The peak related to librational mode of OH^- is detectable in spectra of products formed with mixing molar ratios Ca/P=1.33 and Ca/P=1.67 (around 630 cm^{-1}). Concerning peaks assigned to vibrations of the phosphate group, $PO4^{3-}$, the broadening of the phosphate characteristic bands at 900–1200 cm^{-1} and at 580–603 cm^{-1} may be explained by the small dimensions of HAp particles precipitated (Venkateswarlu et al., 2010). FITR spectra also exhibit carbonate bands, which can be explained by the absorption of CO_2 from air or water, once the reaction system was open to air. Carbonate bands were only observed in the spectra of the precipitates obtained for the larger mixing Ca/P molar ratios (1.33 and 1.67), since alkaline solutions readily absorb CO_2 (Osaka et al., 1991). In addition, carbonate band positions at approximately 1459, 1422 and 875 cm^{-1} for Ca/P=1.33, and at 1424 and 875 cm^{-1} for Ca/P=1.67, seem to indicate that the HAp formed is carbonated HAp of B-type, where the carbonate ions occupy the phosphate ions sites (Landi et al., 2003). Further, presence of a peak around 875 cm^{-1} is detectable in all the spectra. This may indicate the formation of a calcium

deficient HAp, as this peak is characteristic of the hydrogen phosphate group, HPO_4^{2-} (Koutsopoulos, 2002).

Based on the results presented above, the most promising experiment from the point of view of the objectives mentioned is the one with a mixing molar ratio Ca/P=1.33, as stable HAp nanoparticles were obtained under near-physiological conditions of temperature and pH.

3.3. Characterization of the HAp precipitation process for a mixing molar ratio Ca/P=1.33

Supersaturation with respect to HAp, octacalcium phosphate (OCP) and beta-tricalcium phosphate (β-TCP) was calculated based on the ratio between the calcium concentration measured and the calcium concentration at equilibrium (Fig. 5). The equilibrium concentration of calcium was determined using published solubility isotherms of the different calcium phosphate salts for the system $Ca(OH)_2$–H_3PO_4–H_2O at 37 °C (Fernández et al., 1999). According to the existing conditions of pH and supersaturation (Figs. 2 and 5) the calcium phosphate to precipitate should be HAp.

From Fig. 6, three stages can be observed during HAp precipitation with a mixing molar ratio Ca/P=1.33. In stage 1, there is a decrease in pH (from approximately 12 to 8.2) followed by a period of stabilization, and a decrease in calcium concentration. Particles formed seem to be spherical with a diameter of approximately 20 nm and in an amorphous state (Fig. 8). According to XRD results (Figs. 7 and 8), precipitation of amorphous calcium phosphate $Ca_3(PO)_2$ (ACP) occurs, which can be described by the following equation:

$$Ca(OH)_2 + 2H_3PO_4 \rightarrow Ca_3(PO_4)_2 + 6H_2O \quad (2)$$

During stage 2, it seems that transformation of ACP to HAp occurs. In fact, XRD results (Fig. 7) confirmed the presence of HAp. Regarding SEM images (Fig. 9), particles with two distinguished forms are shown, one spherical with a diameter around 20 nm and similar to the particles observed in stage 1, and one more elongated, with approximately 20 nm width and 100 nm long. According to Eq. (3), transformation of ACP to HAp causes consumption of calcium and hydroxide ions, which is experimentally verified (Fig. 6):

$$8Ca3(PO4)_2 + Ca^{2+} + 4OH^- + H_2O \rightarrow 5Ca_5(PO_4)_3OH + HPO_4^{2-} \quad (3)$$

In stage 3, pH and $[Ca^{2+}]$ stabilize, meaning that the majority of the growth process is completed and that the product formed is stable. Fig. 7 confirms that the product formed is HAp, the XRD curves of stage 2 and stage 3 being overlapped. In terms of morphology and size, Fig. 10 shows rod-like particles of about 20 nm width and 100 nm long.

Based on the results presented above, it seems that the precipitation process is characterized by the formation of ACP and its subsequent conversion to HAp. Nevertheless, formation of octacalcium phosphate $5Ca_4H(PO_4)_3$ (OCP) could be expected,

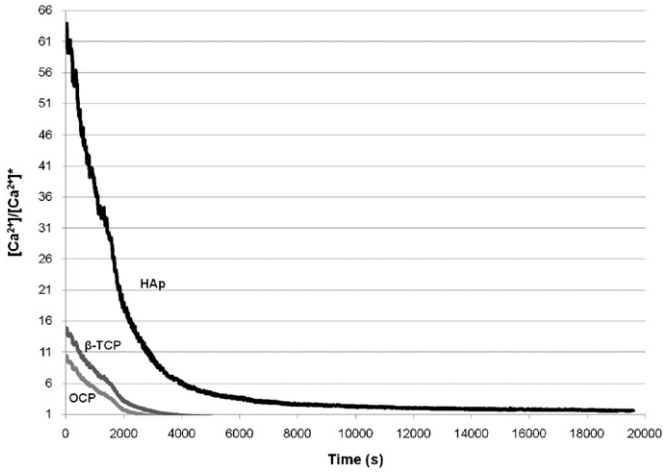

Fig. 5. Variation of supersaturation with time with respect to HAp, OCP and β-TCP.

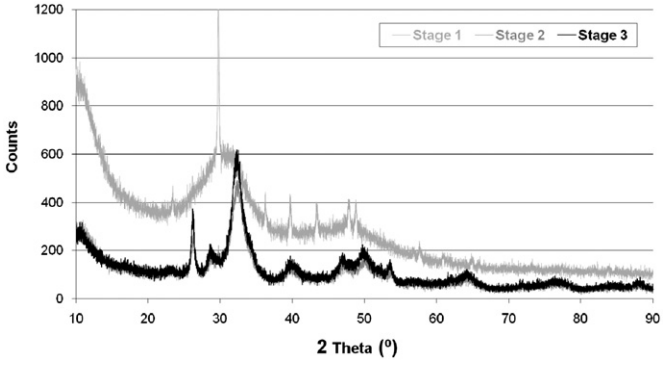

Fig. 7. XRD patterns of the products formed in the different stages of HAp precipitation for a mixing molar ratio Ca/P=1.33.

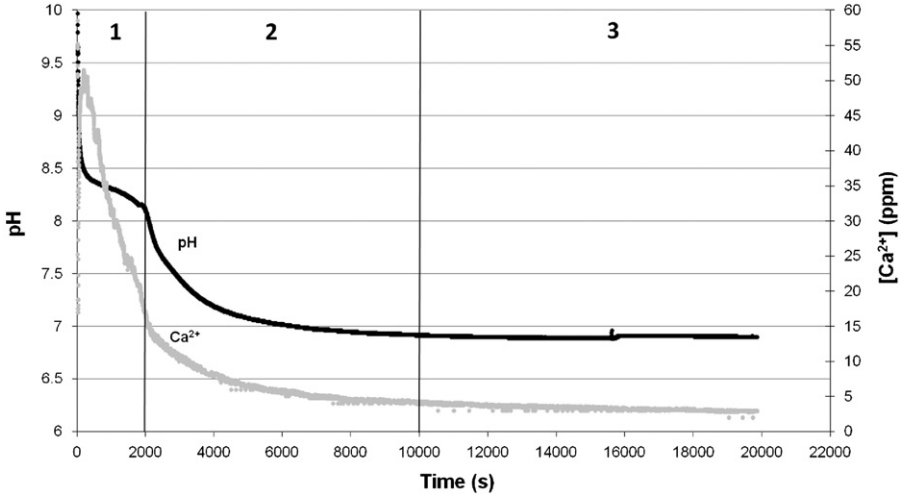

Fig. 6. pH and $[Ca^{2+}]$ variation with time during HAp precipitation for a mixing molar ratio Ca/P=1.33.

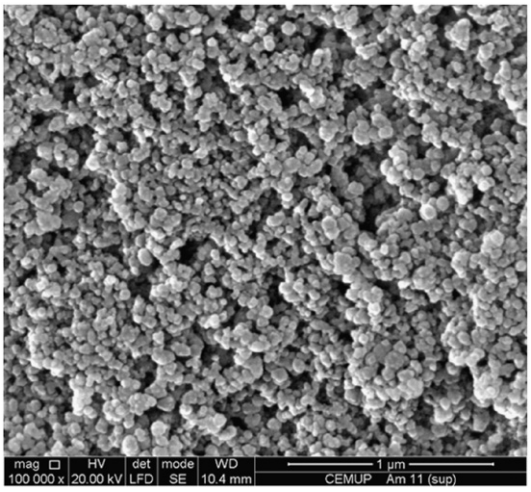

Fig. 8. SEM image of the product formed in stage 1 of HAp precipitation for a mixing molar ratio Ca/P=1.33.

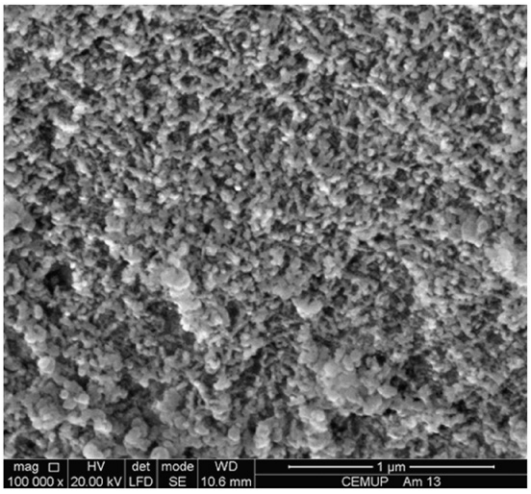

Fig. 9. SEM image of the product formed in stage 2 of HAp precipitation for a mixing molar ratio Ca/P=1.33.

since the system is supersaturated with respect to OCP at the beginning of the experiment (Fig. 5). In the case of OCP being an intermediate phase in the formation of HAp, transformation of ACP to OCP requires an uptake of phosphate and hydrogen ions and a release of calcium into solution, as described below:

$$7Ca3(PO4)_2 + HPO_4^{2-} + 4H^+ \rightarrow 5Ca_4H(PO_4)_3 + Ca^{2+} \quad (4)$$

But this is not confirmed by the experimental data, where a decrease of both calcium concentration and pH is observed. However, the possibility of OCP being a precursor remains, but is so unstable that it is rapidly converted to HAp (Eq. (5)). This may explain the fact that OCP was not detected.

$$6Ca4H(PO4)_3 + Ca^{2+} + 8OH^- \rightarrow 5Ca_5(PO_4)_3OH + 3HPO_4^{2-} + 3H_2O \quad (5)$$

The Ca/P molar ratio of the final product was determined. The product synthesized is characterized by a Ca/P molar ratio of 1.78 ± 0.05, which is higher than the stoichiometric value, thus showing the formation of a carbonated HAp of B-type. From the results obtained, particles precipitated seem to possess characteristics similar to biological apatites, since they are generally considered carbonated of B-type, exhibiting a Ca/P molar ratio higher than 1.67 (Landi et al., 2003; Kumta et al., 2005).

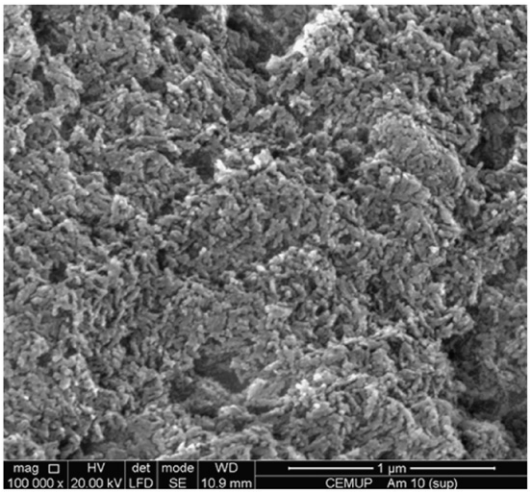

Fig. 10. SEM image of the product formed in stage 3 of HAp precipitation for a mixing molar ratio Ca/P=1.33.

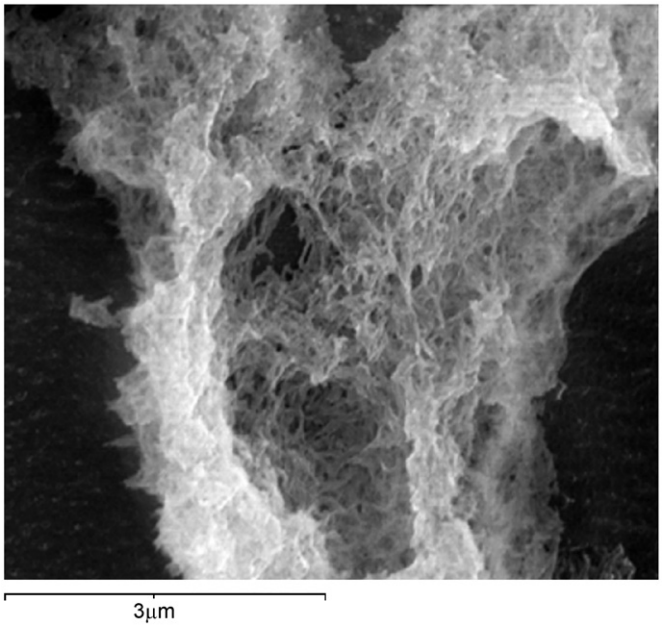

Fig. 11. Cryo-SEM image of the final suspension obtained from the HAp precipitation for a mixing molar ratio Ca/P=1.33.

Finally, final suspensions were characterized in terms of their behavior in solution (cryo-SEM) and in terms of size distribution (laser diffraction). From cryo-SEM image (Fig. 11), it can be seen that HAp particles have the tendency to aggregate in solution, forming micrometric-size clusters, while based on SEM images (Figs. 9 and 10) HAp crystals have a size close to 100 nm. It also can be seen that the structures formed by those clusters have a porous nature. Aggregates of HAp particles with sizes of several microns were also observed by Saeri et al. (2003). The granulometric analysis of HAp particles in volume (Fig. 12a) revealed the formation of aggregates with an average equivalent diameter around 39.5 µm. From the laser analysis in number (Fig. 12b), HAp crystals range in size from 0.052–0.229 µm and have a mean equivalent diameter of 0.128 µm, presenting a narrow size distribution curve, similar to the one presented in Gomes et al. (2009) work. Based on zeta potential measurements (Table 1), suspensions obtained are unstable. In the case of the product formed in stage 1, the aggregation phenomenon can be justified by its amorphous state and the particles dimensions,

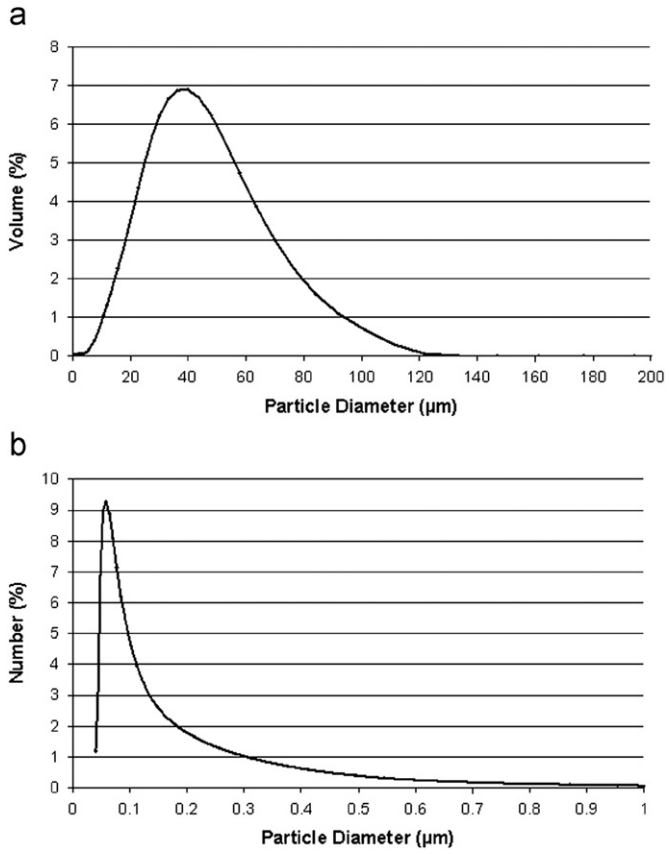

Fig. 12. Particle size distribution of HAp particles obtained from the HAp precipitation for a mixing molar ratio Ca/P=1.33: (a) in volume; and (b) in number.

since they possess a high surface area to volume ratio, resulting in a high surface tension which they tend to lower by adhering to one another. The suspension seems to stabilize during the precipitation, as zeta potential value increases from stage 1 to stage 3. In fact, as crystals grow larger and become more stable, the surface tension decreases. However, zeta potential remains low indicating that the final suspension continues unstable. According to Bouyer et al. (2000), the isoelectric point (IEP) of HAp varies between 4 and 6, and the pH of the final suspension is approximately equal to 7, which is close to the IEP of HAp and can thus explain the instability of the suspension. It is important to refer that zeta potential values are widely dispersed, which is mainly due to the presence of aggregates with different sizes.

4. Conclusion

This study describes a simple approach for the precipitation of HAp nanoparticles at 37 °C. Experiments with different mixing Ca/P molar ratios (1, 1.33 and 1.67) were investigated. Formation of HAp single-phased was confirmed by XDR and FTIR, for all the experimental conditions used. It also has been shown that for the mixing molar ratio Ca/P=1.33, stable HAp nanoparticles were obtained at a pH close to 7, which is particularly important in the preparation of HAp for medical purposes. The precipitation process was characterized, revealing the existence of three stages: precipitation of ACP, transformation of ACP to HAp, and growth of HAp. The final product was characterized by a molar ratio Ca/P=1.78 ± 0.05, which is typical of a carbonated HAp of B-type. In addition, it was shown that the final product was composed of aggregates formed by nanoparticles with a rod-like shape of about 20 nm with and 100 nm long.

Table 1
Zeta potential measurements for the suspensions collected in stages 1 and 3 from HAp precipitation for a mixing molar ratio Ca/P=1.33.

	Suspension collected in stage 1	Suspension collected in stage 3
Zeta potential (mV)	2.99 ± 2.06	18.9 ± 4.1

It is important to highlight that HAp particles produced in this work have characteristics (morphology, size and crystallinity) similar to particles already available in the market. But unlike other works, HAp precipitation was carried out at low temperature and without maintaining a fixed pH, so avoiding the use of additional chemical compounds and experimental steps. Finally, this work can be a useful contribution to other studies, namely because precipitation of HAp was studied in a reaction medium where pH is changing and also because the process was fully characterized, which is important for the understanding of the mechanism of HAp formation.

Acknowledgments

This work was supported by the Portuguese Foundation for Science and Technology (SFRH/BD/42992/2008) through the MIT-Portugal Program, Bioengineering Systems Focus Area. The authors are thankful to Dr. Jorge Ferreira from LNEG (Laboratório Nacional de Energia e Geologia) for carrying out the X-ray measurements and their help with the interpretation of results.

References

Bernard, L., Freche, M., Lacout, J.L., Biscans, B., 2000. Modeling of the dissolution of calcium hydroxyde in the preparation of hydroxyapatite by neutralization. Chem. Eng. Sci. 55 (23), 5683–5692.
Bouyer, E., Gitzhofer, F., Boulos, M.I., 2000. Morphological study of hydroxyapatite nanocrystal suspension. J. Mater. Sci: Mater. Med. 11 (8), 523–531.
Elliot, J.C., 1994. Structure and chemistry of the apatites and other calcium orthophosphates. Elsevier, Amsterdam.
Fernández, E., Gil, F.J., Ginebra, M.P., Driessens, F.C.M., Planell, J.A., Best, S.M., 1999. Calcium phosphate bone cements for clinical applications. Part I: Solution chemistry. J. Mater. Sci.: Mater. Med. 10 (3), 169–176.
Ferraz, M.P., Monteiro, F.J., Manuel, C.M., 2004. Hydroxyapatite nanoparticles: A review of preparation methodologies. J. Appl. Biomater. Biomech. 2, 74–80.
Gomes, P.J., Silva, V.M.T.M., Quadros, P.A., Dias, M.M., Lopes, J.C.B., 2009. A highly reproducible continuous process for hydroxyapatite nanoparticles synthesis. J. Nanosci. Nanotechnol. 9, 3387–3395.
He, Q.J., Huang, Z.L., 2007. Controlled growth and kinetics of porous hydroxyapatite spheres by a template-directed method. J. Cryst. Growth. 300 (2), 460–466.
Johannsen, K., Rademacher, S., 1999. Modelling the Kinetics of Calcium Hydroxide Dissolution in Water. Acta Hydrochim. Hydrobiol. 27 (2), 72–78.
Koutsopoulos, S., 2002. Synthesis and characterization of hydroxyapatite crystals: A review study on the analytical methods. J. Biomed. Mater. Res. 62 (4), 600–612.
Kumta, P.N., Sfeir, C., Lee, D.-H., Olton, D., Choi, D., 2005. Nanostructured calcium phosphates for biomedical applications: novel synthesis and characterization. Acta Biomater. 1 (1), 65–83.
Landi, E., Celotti, G., Logroscino, G., Tampieri, A., 2003. Carbonated hydroxyapatite as bone substitute. J Eur Ceram Soc 23 (15), 2931–2937.
Liu, C., Huang, Y., Shen, W., Cui, J., 2001. Kinetics of hydroxyapatite precipitation at pH 10 to 11. Biomaterials 22 (4), 301–306.
Ma, M.-G., Zhu, J.-F., 2009. Solvothermal Synthesis and Characterization of Hierarchically Nanostructured Hydroxyapatite Hollow Spheres. Eur. J. Inorg. Chem. 2009 (36), 5522–5526.
Marković, S., Veselinović, L., Lukić, M.J., Karanović, L., Bračko, I., Ignjatović, N., Uskoković, D., 2011. Synthetical bone-like and biological hydroxyapatites: a comparative study of crystal structure and morphology. Biomed. Mater. 6.
Osaka, A., Miura, Y., Takeuchi, K., Asada, M., Takahashi, K., 1991. Calcium apatite prepared from calcium hydroxide and orthophosphoric acid. J. Mater. Sci.: Mater. Med. 2 (1), 51–55.
Perry, R.H.,Green, D.W., 1997. Perry's Chemical Engineers' Handbook.
Saeri, M.R., Afshar, A., Ghorbani, M., Ehsani, N., Sorrell, C.C., 2003. The wet precipitation process of hydroxyapatite. Mater. Lett. 57 (24–25), 4064–4069.

Safavi, K., Nakayama, T.A., 2000. Influence of Mixing Vehicle on Dissociation of Calcium Hydroxide in Solution. J. Endod. 26 (11), 649–651.
Tadic, D., Peters, F., Epple, M., 2002. Continuous synthesis of amorphous carbonated apatites. Biomaterials 23 (12), 2553–2559.
van Kemenade, M.J.J.M., de Bruyn, P.L., 1987. A kinetic study of precipitation from supersaturated calcium phosphate solutions. J. Colloid. Interface Sci. 118 (2), 564–585.
Venkateswarlu, K., Chandra Bose, A., Rameshbabu, N., 2010. X-ray peak broadening studies of nanocrystalline hydroxyapatite by Williamson–Hall analysis. Physica B 405 (20), 4256–4261.
Zhou, W., Wang, M., Cheung, W., Guo, B., Jia, D., 2008. Synthesis of carbonated hydroxyapatite nanospheres through nanoemulsion. J. Mater. Sci.: Mater. Med. 19 (1), 103–110.